Anal. Chem. **2007,** *79,* 5217−5224

Hybrid Amperometric and Conductometric Chemical Sensor Based on Conducting Polymer Nanojunctions

Erica S. Forzani, Xiulan Li, and Nongjian Tao*

Department of Electrical Engineering, Arizona State University, Tempe, Arizona 85287

We report on a hybrid chemical sensor that can perform either amperometric or conductometric detection alone or simultaneously. It consists of an array of electrode pairs in which the two electrodes in each pair are separated with micrometer to nanometer-scale gaps. The gaps are bridged with conducting polymer (polyaniline) so that one can measure the conductance of the polymer bridge like a conventional Chem-FET. The electrode geometries are designed to allow simultaneously detection of electrochemical current like a conventional microelectrode amperometric sensor. The hybrid device provides increased selectivity for detection of analytes in complex matrixes and may provide new insights into the electrochemical reaction mechanisms of analytes. As an example, we have demonstrated the detection of dilute neurotransmitter (dopamine) in the presence of its concentrated major physiological interferent, ascorbic acid, which is not possible using either the amperometric or the conductometric techniques alone.

Electrochemical detection principles have been widely used in chemical sensors and biosensors.[1−3] One of the most successful electrochemical techniques is the amperometric method, which detects electrochemical reaction currents related to target analytes.[4,5] Another successful signal transduction mechanism is to detect target species-induced change in the electrical conductance of a sensing element made of materials such as silicon,[6,7] conducting polymers,[8−10] carbon nanotubes,[11,12] metal oxides,[13,14] and metals.[15] These conductometric approaches have shown particular advantages when the size of the sensing element is shrunk down to nanometer scale. Examples include significant improvements in the sensitivity and time response of the sensors, due to the increased surface to volume ratio of the sensing element.[6−9,11,13−15] In addition, the conductivities of many sensing materials may be controlled with a gate voltage in the fashion of field effect transistors (FET), which provide further flexibility for chemical and biosensor applications.[10,16] However, both amperometric and conductometric detections have their intrinsic limitations. Electrochemical detection can be rather selective and sensitive, but they are susceptible to electroactive interferents that also contribute to the measured total electrochemical reaction current. For example, the amperometric method can detect dopamine (Dpm), a neurotransmitter, via measuring the oxidation current of Dpm.[4,17,18] But ascorbic acid (AA) in physiological fluid is more easily oxidized and more concentrated than Dpm and, thus, a serious interferent for electrochemical detection of Dpm.[5,19] The selectivity of conductometric methods relies primarily on specific binding or interaction of a target species onto the sensing materials functionalized with receptor molecules,[8] which is often inadequate due to nonspecific binding.

In this paper, we demonstrate a hybrid amperometric and conductometric device that retains the advantages of both amperometric and conductometric methods while removing some of the serious drawbacks associated with each of them when used alone (Figure 1A). The hybrid device can detect an analyte via either an electrochemical current signal or conductance signal separately or both signals simultaneously. This hybrid approach enhances selectivity for detection of analyte in complex matrixes, even in the presence of interferents with much higher concentrations than the analyte itself. Using the device, we have detected Dpm in the presence of AA at 3 orders of magnitude higher concentration.[19] This capability cannot be achieved using either the amperometric or the conductometric methods alone.

* To whom correspondence should be addressed. E-mail: njtao@asu.edu.

(1) Babkina, S. S.; Budnikov, G. K. *J. Anal. Chem.* **2006**, *61*, 728.
(2) Rogers, K. R. *Anal. Chim. Acta* **2006**, *568*, 222.
(3) Zhao, W.; Xu, J. J.; Chen, H. Y. *Electroanalysis* **2006**, *18*, 1737.
(4) Cui, H. F.; Ye, J. S.; Chen, Y.; Chong, S.-C.; Sheu, F.-S. *Anal. Chem.* **2006**, *78*, 6347.
(5) Hayashi, K.; Iwasaki, Y.; Horiuchi, T.; Sunagawa, K.; Tate, A. *Anal. Chem.* **2005**, *77*, 5236.
(6) Patolsky, F.; Timko, B. P.; Yu, G. H.; et al. *Science* **2006**, *313*, 1100.
(7) Patolsky, F.; Zheng, G. F.; Lieber, C. M. *Anal. Chem.* **2006**, *78*, 4260.
(8) Wanekaya, A. K.; Chen, W.; Myung, N. V.; et al. *Electroanalysis* **2006**, *18*, 533.
(9) Wang, J.; Bunimovich, Y. L.; Sui, G. D.; et al. *Chem. Commun.* **2006**, 3075.
(10) Fabre, B.; Taillebois, L. *Chem. Commun.* **2003**, 2982.
(11) Shi, L.; Yu, C. H.; Zhou, J. H. *J. Phys. Chem. B* **2005**, *109*, 22102.
(12) Star, A.; Tu, E.; Niemann, J.; et al. *Proc. Natl. Acad. Sci. U. S. A.* **2006**, *103*, 921.
(13) Shi, L.; Hao, Q.; Yu, C. H.; et al. *Appl. Phys. Lett.* **2004**, *84*, 2638.
(14) Murray, B. J.; Li, Q.; Newberg, J. T.; Hemminger, J. C.; Penner, R. M. *Chem. Mater.* **2005**, *17*, 6611.
(15) Im, Y.; Lee, C.; Vasquez, R. P.; et al. *Small* **2006**, *2*, 356.
(16) Forzani, E. S.; Li, X. L.; Zhang, P. M.; et al. *Small 2*, **2006**, 1283.
(17) Wightman, R. M. *Science* **2006**, *311*, 1570.
(18) Heien, M.; Johnson, M. A.; Wightman, R. M. *Anal. Chem.* **2004**, *76*, 5697.
(19) Roy, P. R.; Saha, M. S.; Okajima, T.; et al. *Electroanalysis* **2004**, *16*, 1777.

10.1021/ac0703202 CCC: $37.00
Published on Web 06/12/2007

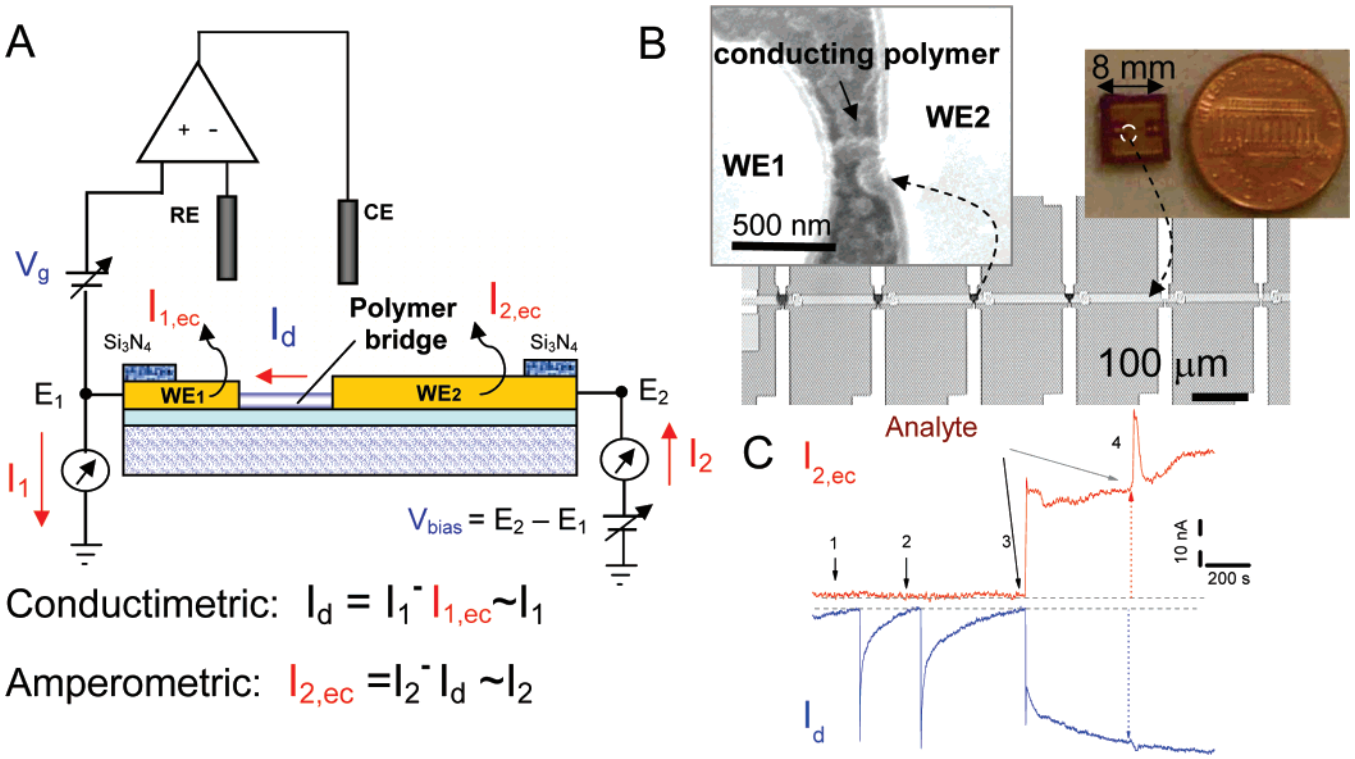

Figure 1. (A) Schematic illustration of a hybrid amperometric and conductometric sensor. WE_1 and WE_2 represent two working electrodes (source and drain electrodes) connected with a conducting polymer bridge. RE and CE are reference and counter electrodes, respectively. The electrochemical gate potential ($V_g = E_1$) is applied between the drain electrode (WE_1) and RE, and a bias voltage (V_{bias}) is applied between WE_1 and WE_2. (B) Optical and scanning electron microscope images of the device made of an array of polymer bridges on a silicon chip. (C) Simultaneous conductometric (I_d) and amperometric ($I_{2,ec}$) detection of HQ. The first 2 injections (labeled "1 and 2") are supporting electrolyte. The injections of HQ (labeled "3 and 4") induce increases in $I_{2,ec}$ due to the oxidation of HQ to quinone (Q) (or HQ → Q + 2e + $2H^+$) and decreases in I_d due to the oxidation of the polymer bridge by the reaction product, Q. V_g (E_1) = 0.2 V, V_{bias} = 0.25 V. See text for details.

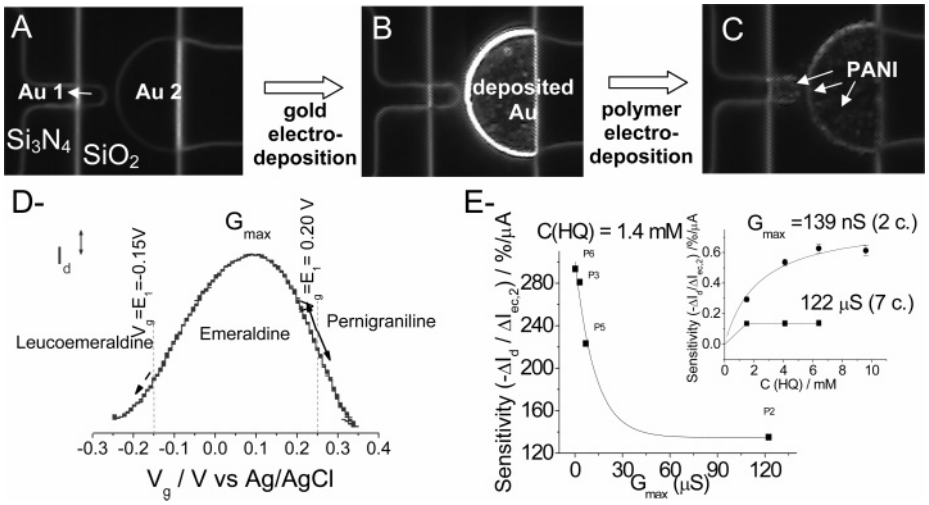

Figure 2. Dark-field optical images of (A) a bare electrode pair, (B) electrode pair after Au electrodeposition onto WE_2, (C) Au electrodeposited electrode pair after the formation of polyaniline nanojunction, (D) I_d vs V_g curve of polyaniline nanojunction in supporting electrolyte (forward swept at 60 mV/s), and (E) sensitivity of the amperometric−conductometric device ($\Delta I_d/\Delta I_{2,\,ec}$) as a function of G_{max}, which measured the amount of polymer deposition. Labels, P2−P6, represent 4 different devices. Inset: sensitivity of two devices as a function of HQ concentration.

EXPERIMENTAL SECTION

Device Fabrication. We used a 360-μm-thick Si (100) wafer (7−13 Ω. cm resistivity) covered with a 50-nm thermal SiO_2 insulation layer. We then patterned the Si substrate with an array of Au electrode pairs using standard photolithography tools (Figures 1B and 2A). The separation between the two electrodes in each pair was ∼ 1−2 μm. The Au electrodes were thermally evaporated with a thickness of 60−100 nm on top of ∼8-nm Cr adhesion layer. A 400-nm-thick Si_3N_4 layer was deposited by chemical vapor deposition on the entire wafer except for a 10-μm-wide strip that exposes the gap regions of all the electrode pairs. The Si_3N_4 layer served as an insulation layer to minimize leakage current due to ionic conduction, which is important for carrying out electrical measurement in electrolytes. The leakage

current was typically a few picoamperes. In order to decrease the gap between the two Au electrodes in each pair, we electrochemically deposit Au onto one of the two electrodes using a method reported elsewhere.[20] A Pt coil and a Ag wire were used as counter electrode and as quasi-reference electrode, respectively. The quasi-reference electrode was calibrated against the more commonly used Ag/AgCl (in 3.0 M KCl). The electrode potentials were controlled using a homemade bipotentiostat. The electrodeposition of Au was carried out by holding the electrode potential at ~ −0.35 V versus Ag/AgCl 0.4 M citric acid (pH 4) containing 10 mM $NaAu(S_2O_3)_2$. During the electrodeposition process, the current between the two electrodes was monitored continuously. Initially, the current was small and entirely due to ionic leakage current. The process was performed at different time deposition to obtain a different gap size.

Polymer Deposition. After completing the fabrication of the electrodes, we thoroughly rinsed the chip with 18 MΩ. cm water to remove Au deposition solution and dried it out with N_2 gas. The device was transferred to a probe station with a hydrophobic cell made by PDMS on top of the device. Polyaniline was deposited onto the electrodes by sweeping the electrode potentials between 0 and 0.9 V (vs Ag/AgCl) at 50−70 mV/s in 0.12 M aniline + 0.5 M H_2SO_4 + 0.13 M $NaHSO_4$+ 2.7 mg/mL poly(4-styrenesulfonate) (7000 g mol^{-1}). The bias voltage applied between two working electrodes was 10−50 mV using the homemade bipotentiostat. When the growing polyaniline strands started to bridge the gap, the current increased sharply. By controlling the number of potential cycles before stopping the deposition process, different amounts of polyaniline bridged between the gaps were obtained. After fabrication of the polymer bridge, the entire chip was then gently rinsed with DI water.

Amperometric−Conductometric Sensor Measurements. We performed the amperometric and conductometric measurements using the homemade bipotentiostat. The bipotentiostat was used to control the potential of the two electrodes in each pair with respect to the quasi-reference electrode. It also has a current amplifier for amperometric detection. To perform the conductometric measurement, we used an electrometer (Keithley, model 617). All measurements described here were carried out in 50 mM H_2SO_4 to demonstrate the concept of the hybrid amperometric−conductometric device. However, other conducting polymer materials work at or near neutral pH (pH 7.2−7.4).[21]

RESULTS AND DISCUSSION

Principle of the Hybrid Device. We describe here briefly the working principle of the device. The key component of the device is a pair of asymmetric working microfabricated electrodes (WE_1 and WE_2) on the silicon chip, one (WE_2) has a much larger (>20 times) area than the other one (WE_1) (Figure 1A). The two electrodes are separated by a gap varying from a few hundreds to a few tens of nanometers, which is bridged with conducting polymer. This electrode design, based on the following consideration, allows one to simultaneously measure the conductivity of the polymer bridge and the current due to electrochemical reactions of analytes taking place on WE_2. The potentials of WE_1 and WE_2 are independently controlled with respect to the quasi-reference electrode using the bipotentiostat, and the associated currents, I_1 and I_2, of the two electrodes are monitored. The potential difference, $E_2 - E_1 = V_{bias}$, is the bias voltage between the two electrodes, which drives a current, I_d, through the polymer bridge. This current (I_d) measures the conductivity of the polymer bridge, which is related to I_1 and I_2 by $I_1 = I_d + I_{1,ec}$ and $I_2 = I_d + I_{2,ec}$, where $I_{1,ec}$ and $I_{2,ec}$ are currents due to electrochemical reactions. We minimize the electrode area of WE1 so that $I_{1,ec} \sim 0$. So $I_d \sim I_1$ gives the conductivity of the polymer bridge (conductometric) and $I_{2,ec} \sim I_2 - I_d$ measures the electrochemical reaction current (amperometric). Since the device operation is analogous to an electrochemically gated field effect transistor, I_d in this paper is also referred to as the drain current.

Many electrochemical reaction schemes can induce changes in I_d and $I_{2,ec}$. In the present paper, we analyze two cases: (1) Independent amperometric−conductometric detection. The analyte, such as AA, is electrochemically active and irreversible. When AA arrives at the device surface, it is electrochemically oxidized and the associated oxidation current through WE_2 is detected. In the meantime, AA interacts with the polymer, which changes the conductivity of the polymer bridge due to the reducing property of AA (see scheme in Figure 3C and details below). (2) Dependent amperometric−conductometric detection. The analyte is electrochemically active and quasi-reversible. Dpm and hydroquinone (HQ) are two examples studied here. As with the first case, Dpm and HQ can be oxidized electrochemically and are detected in amperometric mode. However, unlike the previous case, Dpm and HQ do not affect the conductivity of the polymer bridge. Instead, the reaction products, dopaminequinone (DQ) and quinone (Q), of the two analytes are detected on the polymer bridge due to the changes in the redox activity of the polymer by the reaction products. Figure 1C shows an example of simultaneous measurement of I_d and $I_{2,ec}$ upon successive injections of supporting electrolyte (1−2) and HQ (3−4). The injections of supporting electrolyte cause only transient spikes in the currents due to mechanical disturbance, but the injections of HQ induce increases in $I_{2,ec}$ due to the oxidation of HQ to Q at WE_2 and decreases in I_d values as the reaction product, Q, tends to oxidize the polymer (see below).

Optimization of Amperometric−Conductometric Device. In order to achieve the best performance of the hybrid device, several device parameters were optimized. First, as we have discussed already, small WE_1 and large WE_2 are preferred. This is because small WE_1 (area) reduces electrochemical current on WE_1, so that I_1 is essentially the same as the drain current that measures the conductivity. A relative large WE_2 is important since it collects the electrochemical current, which is proportional to the area of the electrode (Figure 1A).

Second, the size of the gap between the two electrodes is a key to reach low detection levels and fast response in the conductometric mode. We have demonstrated picomolar-range detection limit (ppt)[22] and few-millisecond time response[23] for detection of heavy metal ions[22] and glucose[23] by using polymer bridges of few tens of nanometers. The starting gap size of the microfabricated electrodes in the present work was 2 μm, which was further reduced by selectively depositing metal on WE_2.[20] This

(20) He, H. X.; Li, X. L.; Tao, N.; et al. *J. Phys. Rev. B* **2003**, *68*.
(21) Kim, B.-H.; Diaz, A.; Forzani, E. S.; et al. unpublished results.
(22) Aguilar, A. D.; Forzani, E. S.; Li, X. L.; et al. *Appl. Phys. Lett.* **2005**, *87*.
(23) Forzani, E. S.; Zhang, H. Q.; Nagahara, L. A.; et al. *Nano Lett.* **2004**, *4*, 1785.

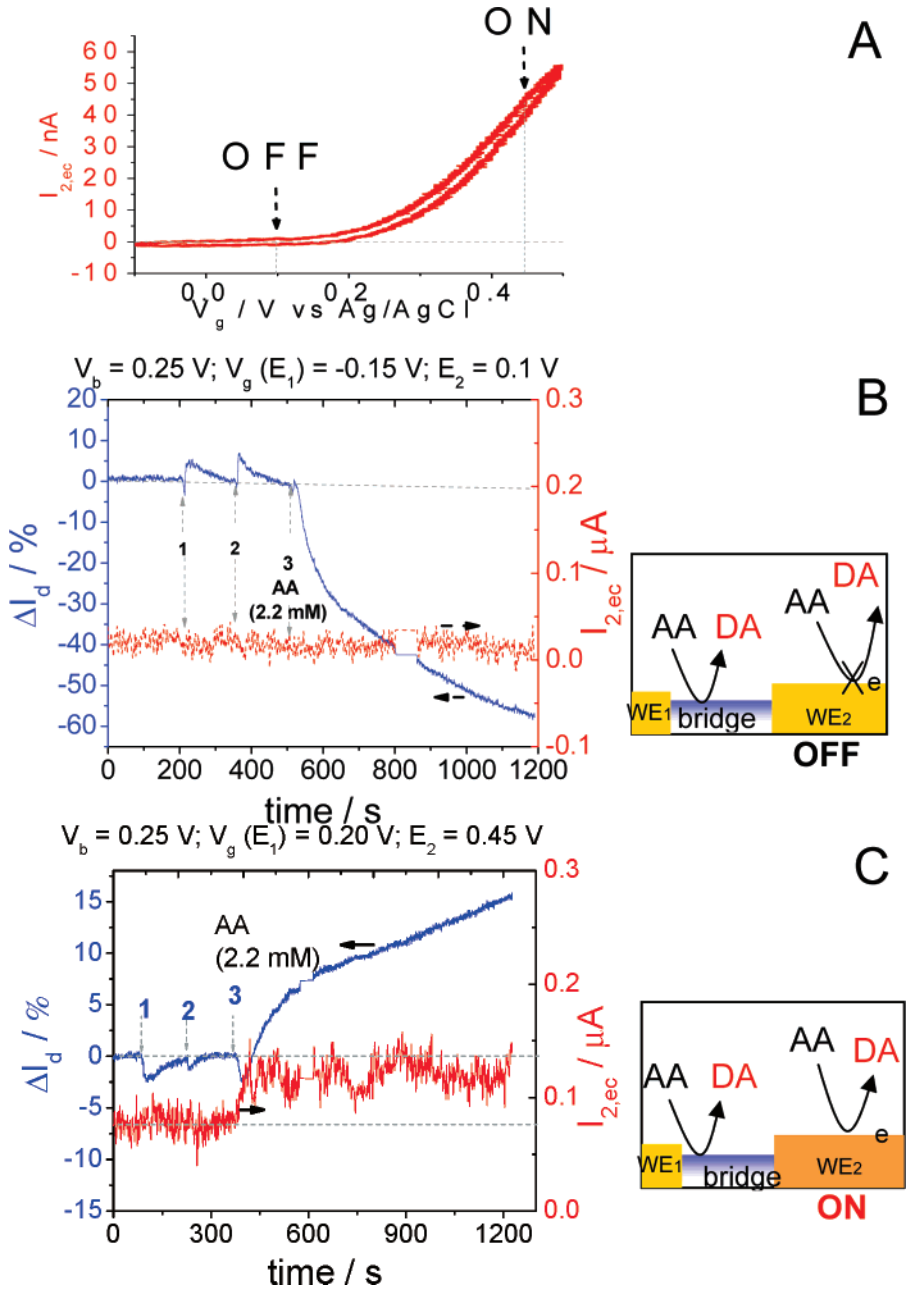

Figure 3. Independent amperometric−conductometric detection. (A) Cyclic voltammogram (I_{ec} vs V_g) of 2.2 mM AA on polyaniline-modified microelectrode (WE_2) at 60 mV/s. and V_{bias} = 0 V. (B, C) Simultaneous recordings of I_d (blue) and $I_{2,ec}$ (red) with the amperometric mode turned "off" (B) and "on" (C) by holding WE_2 at 0.1 and 0.45 V, respectively. Insets in (B) and (C) illustrate the corresponding reaction mechanisms, where DA is dehydroascorbic acid. The first two injections are supporting electrolyte and the third one is AA. Data shown in (B) and (C) were recorded with V_{bias}= 0.25 V.

method has allowed us to control the gap size from micrometers down to a few nanometers. Figure 2A,B shows dark-field optical images of a device before and after electrodeposition of Au, which shows a decreased electrode gap and roughened WE_2 (larger electrode). Figure 2C shows images of the same device after the formation of the polymer nanojunction (bridge). The best gap sizes have been defined between hundreds of nanometers and tens of nanometers for HQ or dopamine detection (Figure 1B). Smaller gaps allow us to fabricate small polymer bridges, which give higher sensitivity in the conductometric mode because of the large surface to volume ratio of polymer material. It also allows electrochemical reaction products generated at the relative large WE_2 to quickly diffuse and reach the entire polymer bridges for conductometric measurements.

We have studied the dependence of the device sensitivity on the polyaniline bridge size. The conductance of polyaniline obtained at small bias voltage (V_{bias}) is strongly dependent on the potentials of the electrodes (E_1 and E_2). Note, at a small bias voltage, E_1 and E_2 are about the same. Figure 2D shows the drain current of a polymer nanojunction as a function of E_1 (V_g) at a constant bias voltage. At low gate potentials, the polymer is in the reduced state (leucoemeraldine), which is insulating, and the conductance (I_d) is small. The conductance increases with the increase of gate potential (V_g or E_1) as the polymer is transformed

into the conducting oxidized state (emeraldine). Further increasing the gate potential oxidizes the polymer to a second insulating state (pernigraniline), which results in a decrease in the conductance.[24] G_{max}, the maximum conductance of the polymer bridge, provides a good measure of the size of the polymer bridge. We fabricate the polymer bridge by cycling the potentials of the electrodes in the presence of aniline. The potential cycling polymerizes aniline into polyaniline and deposits the polymer across the electrodes. By controlling the number of potential cycles (c.), we can control the size of the polymer bridge.

One way to characterize the sensitivity of the conductometric mode is to determine $\Delta I_d/\Delta I_{2,ec}$ at a constant HQ concentration, where the ΔI_d is the change due to Q (HQ electrochemical product) reaction on the polymer, and $\Delta I_{2,ec}$ is the electroxidation current of HQ (Figure 1C). For a given set of electrodes of constant geometry, $\Delta I_{2,ec}$ is constant if the HQ concentration and electrode potentials are fixed, but ΔI_d depends on the size of the polymer bridge. We found that $\Delta I_d/\Delta I_{2,ec}$ increases rapidly when the amount of polymer bridging the gap decreases (Figure 2E). This observation can be attributed to the large surface to volume ratios for small polymer bridges. This trend was observed at different HQ concentrations (inset of Figure 2E).

In addition to optimizing the device geometry for sensitive and selective detection of analytes, we can also tune the performance of the device by adjusting the potentials of the electrodes. The potentials control the conductance of the polymer nanojunctions via control of the redox state of the conducting polymer (Figure 2D). They also control electrochemical reactions of analytes on the two electrodes. The potential difference is the bias voltage, which allows one to control the drain current. By adjusting the potentials, one can optimize the selectivity of the device for detecting an analyte in a complex matrix. We describe below how one may achieve selective detection of Dpm in the presence of high-concentration AA by properly controlling the potentials and by combing the amperometric and conductometric methods. Such a hybrid approach may also provide new insight into the reaction mechanisms of analytes.

Case A: Independent Amperometric−Conductometric Detection. Detection of Ascorbic Acid. Figure 3A shows a cyclic voltammogram ($I_{2,ec}$ vs V_g) of 2.2 mM AA on a polyaniline-modified microelectrode (WE_2), where the rapid increase near 0.2 V (vs Ag/AgCl) in current is due to the oxidation of AA. First, we show the detection of AA by operating the device at the conductometric mode alone (Figure 3B). This was achieved by holding the potentials ($E_1 = V_g = -0.15$ and $E_2 = 0.10$ V) of the two electrodes well below the AA oxidation potential so that no appreciable amount of electrochemical current was detected. We started the experiment by injecting supporting electrolyte into the sample cell and found some small transient changes in I_d and $I_{2,ec}$ due to mechanical disturbance. When AA was injected, I_d decreased monotonously (Figure 3B, blue curve) while $I_{2,ec}$ remained unchanged (Figure 3B, dotted red curve). The decrease in I_d is because AA tended to reduce polyaniline, which decreased the conductivity when holding the potential on the left of the bell curve maximum at E_1 (or V_g) = −0.15 V (Figure 2D, left side arrow, downward direction). Second, we show the operation of the device

(24) Ofer, D.; Crooks, R. M.; Wrighton, M. S. *J. Am. Chem. Soc.* **1990**, *112*, 7869.

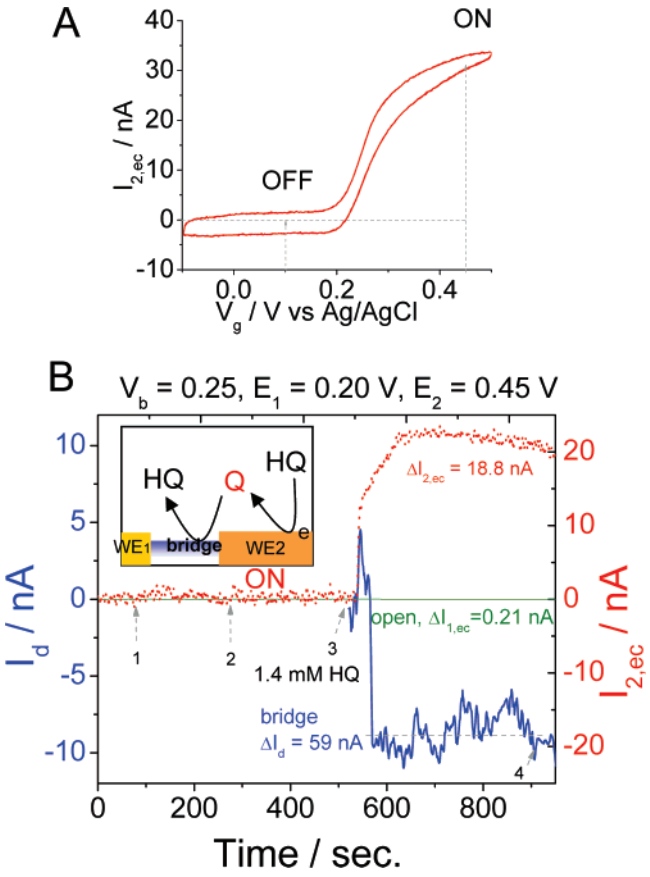

Figure 4. Dependent amperometric−conductometric detection. (A) Cyclic voltammogram of 3.9 mM HQ on polyaniline-modified microelectrode at 60 mV/s. (B) I_d and $I_{2,ec}$ simultaneously recorded during the injections of supporting electrolyte (1−2) and 1.4 mM HQ (3) to a close (bridge) and open polymer bridge (open) amperometric and conductometric device. V_{bias}= 0.25 V and E_2 = 0.45 V. Inset of (B) illustrates the reaction mechanism in a close polymer bridge device.

with both the conductometric and amperometric modes turned on. Figure 3C shows simultaneous detection of I_d and $I_{2,ec}$ ($E_1 = V_g = 0.20$ V and $E_2 = 0.45$ V). In this case, $I_{2,ec}$ increased upon AA injection due to electrochemical oxidation of AA on WE_2 (Figure 3C, red curve). In parallel, an increase in I_d was also observed (Figure 3C, blue curve). The observed increase in the conductivity is because the device was operated on the right side of the bell curve maximum at E_1 (or V_g) = 0.2 V and AA reduces the polymer (Figure 2D, right side arrow, upward direction). These experiments indicate that AA can be detected by operating the hybrid device either in the conductometric or the amperometric mode alone.

Case B: Dependent Amperometric−Conductometric Detection. We now turn to the case where the analytes by themselves do not affect the conductivity of the polymer bridges, but their reaction products can interact with and change the conductivity of the polymer bridges. In other words, we must turn on the amperometric mode in order to use the conductometric mode in this case. This dependent operation can provide better discrimination against possible interferents.

Detection of HQ or Dpm. Figure 4A is a cyclic voltammogram of 3.9 mM HQ on a polyaniline-modified microelectrode, which shows a large increase in current, due to the electrooxidation of HQ, when increasing potential above 0.2 V. The reaction pathway

is given by HQ → Q + 2H$^+$ + 2e, which is quasi-reversible. Figure 4B shows the simultaneously recorded I_d and $I_{2,ec}$ as a function of time. During the experiment, E_1 (V_g) was held at 0.2 V so that no HQ oxidation took place on WE$_1$, while E_2 was fixed at 0.45 V to allow electrooxidation of HQ taking place on WE$_2$. Upon injection of 1.4 mM HQ, $I_{2,ec}$ increases sharply due to the electrooxidation and then reaches a plateau (Figure 4B, red curve). The simultaneously recorded I_d shows a sudden decrease (Figure 4B, blue curve), which may be understood based on the following considerations. The potentials of the two electrodes were held at the right side of the bell curve maximum (Figure 2D). When HQ oxidizes on WE$_2$, the reaction product Q is an oxidizing agent that diffuses to the polymer bridge and shifts the polymer toward the pernigranilline state (see Figure 2D). Consequently, the conductivity (or I_d) decreases.

We note that I_d was determined from I_1, the current through WE$_1$, by assuming $I_{1,\,ec}$, the electrochemical reaction component of I_1 to be small. In order to confirm the assumption, we have performed the measurement with a broken polymer bridge between the two electrodes so that no drain current ($I_d = 0$) is possible. In this case, $I_1 = I_{1,ec} + I_d = I_{1,ec}$, so I_1 solely measured the electrochemical component, $I_{1,\,ec}$. We found that $I_{1,ec}$ was indeed negligibly small (less than a few hundred pA) (Figure 4B, "open" curve).

Detection of HQ in the Presence of AA. In order to demonstrate that the hybrid device can detect mixed analytes, we have studied Dpm and HQ in presence of AA. Figure 5 shows the changes in both, the conductivity (or I_d) of a polyaniline bridge and electrochemical current ($I_{2,ec}$) through WE$_2$. During the measurements, the potentials of the two electrodes were held at $E_1 = 0.20$ V and $E_2 = 0.45$ V (V_{bias}= 0.25 V). Again, mechanical disturbance associated with the injections of supporting electrolyte caused only transient changes in the measured drain and electrochemical reaction currents. The injections of pure HQ induced an increase in the electrochemical current ($I_{2,ec}$) and a decrease in the drain current (conductivity) (Figure 5A). The injections of AA also resulted in an increase in $I_{2,ec}$ due to electrochemical oxidation of AA but an increase in the drain current for the reason discussed earlier (Figure 5B). In the case of mixed AA and HQ, the measured electrochemical current (amperometric) is a result of oxidation of both AA and HQ. The drain current change reflects the competition between the tendency of an increase in the current by AA and decrease by HQ (Figure 5C). When AA is low in concentration, ΔI_d is negative since HQ dominates. However, increasing AA concentration, ΔI_d turns into positive as AA becomes dominant. So the amperometric measurement gives the overall amount of AA and HQ, while the conductometric data measure the relative difference in the concentrations of the two analytes. The ratio, $\Delta I_d/\Delta I_{2,ec}$, versus relative concentration of the two analytes (C_{HQ}/C_{AA}) is shown in Figure 5D (note that the C_{HQ}/C_{AA} scale is nonlinear). Results from other devices are similar. Using the plot such as the one shown in Figure 5D, one can extract relative concentrations of two analytes from experimental $\Delta I_d/\Delta I_{2,ec}$ ratios. The experiment shows that the hybrid device can detect two electroactive analytes in a mixed medium.

Detection of Dpm in the Presence of High Concentrations of AA. The amperometric method has been used to monitor neurotransmitters such as Dpm through oxidation currents.[17,18] One of the major difficulties is the presence of a large amount of AA, which is also oxidizable.[5,19] To demonstrate the usefulness of the hybrid sensor, we performed detection of dilute Dpm (hundreds nM–few μM range) in the presence of highly concentrated AA (1–2 mM range). Figure 6A shows the time course of simultaneous amperometric and conductometric operations with the hybrid device. Dpm was successively injected in the presence of 3 orders of magnitude more concentrated AA. As before, initial injections of supporting electrolyte are performed to monitor the stability of the conducting bridge toward injections (1–3) to ensure no significant changes in the currents due to mechanical disturbance of solution injections. After that, AA was injected to bring AA concentration to the level of millimolar range (4), which causes larges increases in both I_d and $I_{2,ec}$. After I_d and $I_{2,ec}$ reached steady states, Dpm was injected (5–7). Since AA is much more concentrated (~10^3) than Dpm, the injection of Dpm did no result

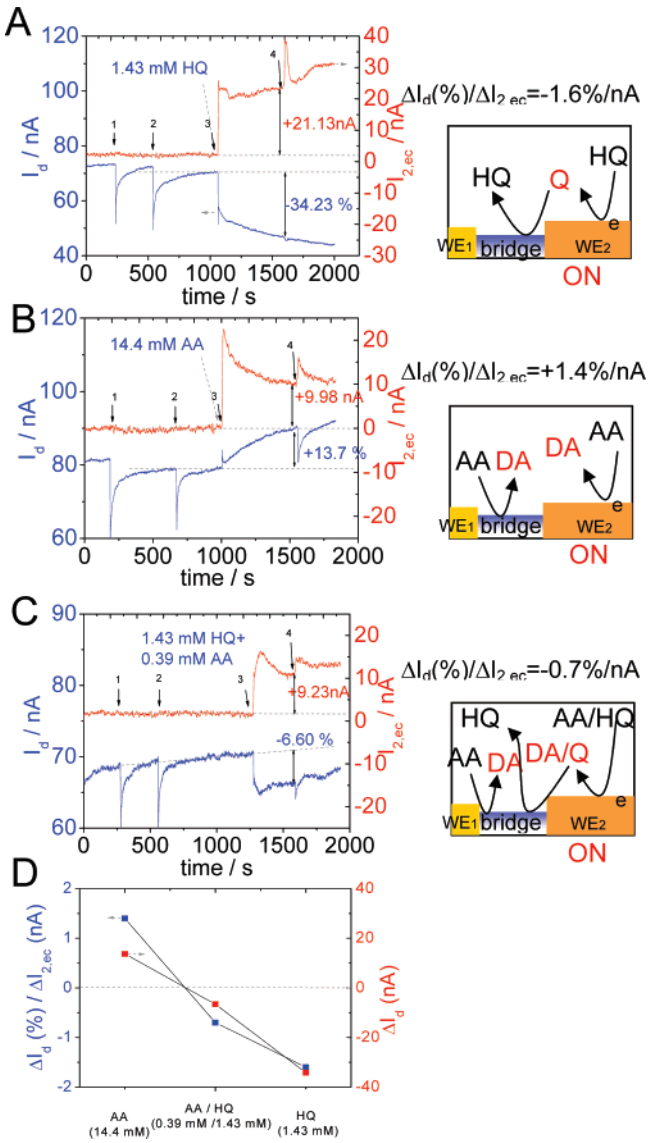

Figure 5. Amperometric–conductometric detections of HQ (A), AA (B), and a mixture of HQ and AA (C). V_{bias}= 0.25 V, and E_2 = 0.45 V. Labels 1 and 2 are injections of supporting electrolyte, and labels 3 and 4 are injections of the analytes. (D) $\Delta I_d/\Delta I_{2,ec}$ and ΔI_d vs AA/HQ concentration ratio. Insets in (A–C) illustrate the reaction mechanisms.

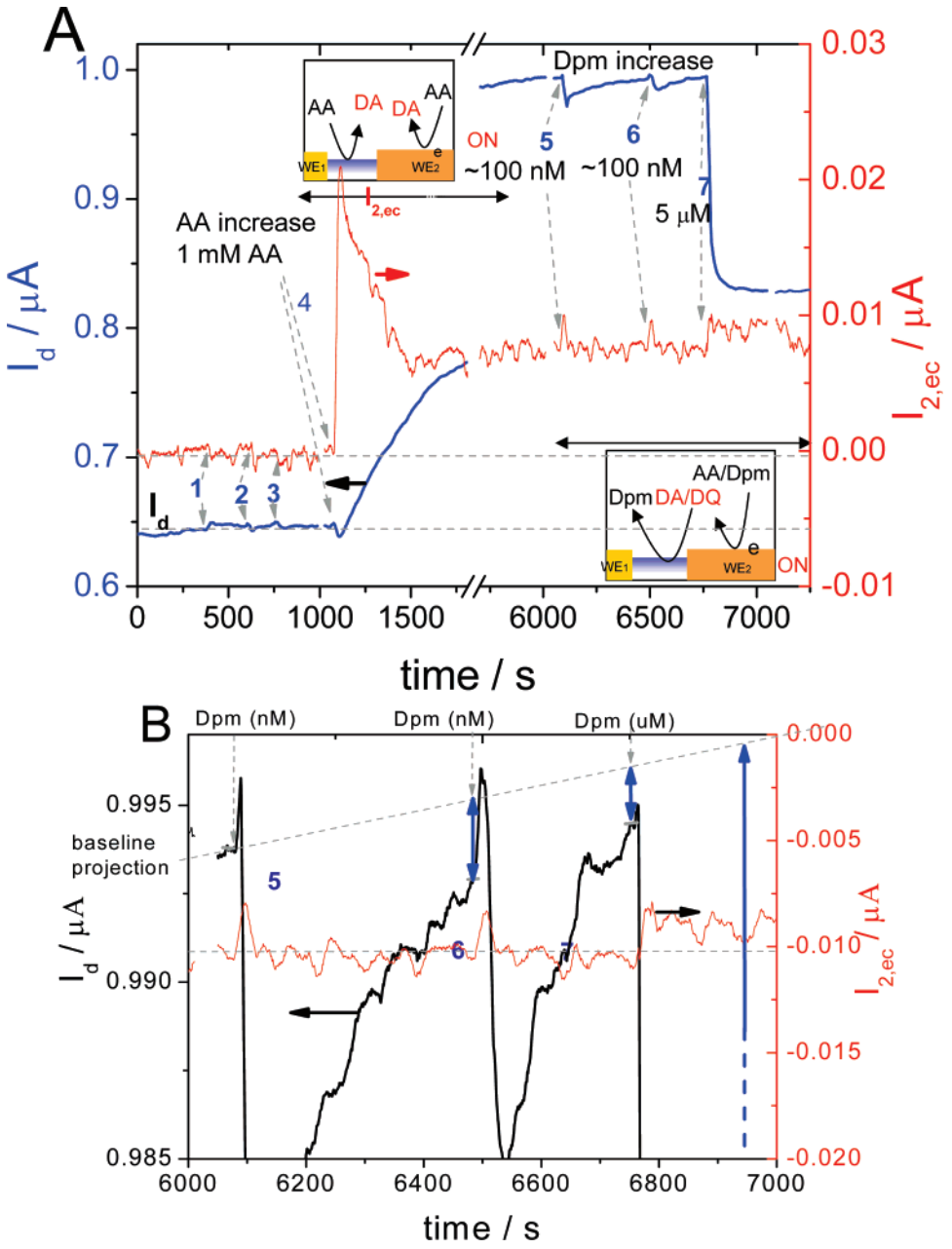

Figure 6. Application of the hybrid sensor to detect neurotransmitter Dpm, in presence of a major physiological interferent, AA, at a concentration level 3 orders of magnitude higher than Dpm. Electrochemical current ($I_{2,ec}$) and drain (I_d) current are monitored simultaneously upon injections of supporting electrolyte (labeled 1−3), AA (labeled 4, Dpm (labeled 5−7). $V_g = 0.45$ V, and $V_{bias} = 0.25$ V. (B) Zooming-in of the curve showing more clearly the Dpm-induced conductivity changes. Insets in (A) illustrate the reaction mechanisms.

in a measurable amount of change in the electrochemical current ($I_{2,ec}$) (Figure 6A,B). However, the electrochemical product of Dpm (dopaminoquinone) even at relatively low concentration causes significant change in the conductivity of the polymer bridge (see inset scheme in Figure 6A). The experiment demonstrated that dilute or small changes in Dpm (≥100 nM) can be detected continuously in the presence of a major physiological interferent (AA) (~ 1 mM) with the hybrid amperometric−conductometric device.

CONCLUSIONS

We have demonstrated a hybrid device that can detect analytes using either conductometric or amperometric mode, or both modes simultaneously. The device consists of an array of conducting polymer nanojunctions; each nanojunction is polyaniline bridged between two electrodes. By carefully designing and optimizing the electrode geometries and separations, the device allows conductivity and electrochemical reaction current to be detected independently. It overcomes many drawbacks associated with the conventional electrochemical and conductometric (or Chem-FET) sensors. The major advantages of the hybrid device include the following: (a) improved selectivity and sensitivity over devices based on either amperometric or conductometric detection alone; (b) detection of an analyte in the presence of interferents at orders of magnitude of higher concentrations; (c) integration of both detection methods (amperometric and conductometric)

using an array of many parallel devices on a single chip, which promises a miniaturized sensor for detecting multiple analytes.

We have illustrated the applications of the hybrid device using Dpm and HQ in the mixed medium with AA. We anticipate that the hybrid approach will lead to other chemical or biochemical applications for detection of analytes in gas phase, cultures, and tissues.

ACKNOWLEDGMENT

This work is supported by NSF (CHM-0554786).

Received for review February 14, 2007. Accepted May 7, 2007.

AC0703202